Visual Neuroscience (1995), **12**, 743–754. Printed in the USA.

Sensitivity to full-field visual movement compatible with head rotation: Variations among axes of rotation

LAURENCE R. HARRIS AND LORI A. LOTT
Department of Psychology, York University, Toronto, Ontario M3J 1P3, Canada

(RECEIVED October 5, 1994; ACCEPTED January 9, 1995)

Abstract

Movement detection thresholds for full-field visual motion about various axes were measured in three subjects using a two-alternative forced-choice staircase method. Thresholds for 1-s exposures to rotation about different rotation axes varied significantly over the range 0.139 ± 0.05 deg/s to 0.463 ± 0.166 deg/s. The highest thresholds were found in response to rotation about axes closely aligned to the line of sight. Variations among the thresholds for different axes could not be explained by different movement patterns in the fovea or variations in motion sensitivity with eccentricity. The variations can be well simulated by a three-channel model for coding the axis and velocity of full-field visual motion. A three-channel visual coding system would be well suited for extracting information about self-rotation from a complex pattern of retinal image motion containing components due to both rotation and translation. A three-channel visual motion system would also be readily compatible with vestibular information concerning self-rotation arising from the semicircular canals.

Keywords: Visual motion, Full-field motion, Visual detection thresholds, Self motion, Channels

Introduction

The correct interpretation of visual motion on any one part of the retina depends on the pattern of motion over the entire visual field. If motion only occurs in one spot, it is probably due to external movement. On the other hand, movement of the entire retinal image in an orderly fashion is a reliable indicator that the eye itself is moving relative to the visual scene. Movements of the eye can take the form of rotation within the orbit or can be produced by rotation or translation of the head. A rotation of the head—necessarily around an axis that does not pass through both eyes—has both rotational and translational consequences for the eyes. The rotational consequence of eye movement is the retinal image moving as a unit with no relative movement between the images of objects at different distances from the viewer. In contrast, translation of the eye results in more complex retinal movement in which the movement of the image of each part of each object depends on its distance from the viewer and its direction with respect to the direction of translation (see Harris, 1994 for a review). During normal life, therefore, the retinal image will contain motion due to three sources: rotation of the eye, translation of the eye, and external movement. In this paper, we propose a simple model, specialized for the processing of full-field motion due to rotation of the eye. The model's operation would be insensitive to simultaneous translation or external movement. The extraction of rotation information from the complex pattern of visual motion normally present on the retina is extremely useful for several important functions. These include assessing orientation in space, distinguishing visual information due to self-motion and also easing the computational burden of using visual motion to assess translation.

Sensitivity to full-field motion, when there is no relative motion within the retinal image but only motion of a pattern as a whole across the retina, is much lower than sensitivity to movement when there are stationary reference points. A typical lower motion threshold for detecting the motion of a spot moving in the presence of a frame is 0.03 deg/s (Johnston & Wright, 1985) but up to a factor of 10 higher for motion with no reference points (Choudhury & Crossey, 1981; Johnson & Scobey, 1982; Snowden, 1992; Howard & Howard, 1994 and see below). This in itself suggests a separate mechanism for the processing of full-field movement.

Object motion, in common with many other aspects of visual processing, is probably carried out by a channel-based system (Levinson & Sekuler, 1976). A psychophysical channel system consists of a set of channels each tuned to a particular value of a stimulus dimension (e.g. velocity) that covers the operating range for that parameter. Each channel is maximally sensitive to a particular value and its sensitivity falls off for values greater or smaller than this optimum. A particular stimulus will thus activate each channel to an extent proportional to its sen-

Reprint requests to: Laurence R. Harris, Department of Psychology, York University, Toronto, Ontario M3J 1P3, Canada.
Present address of Lori A. Lott: College of Optometry, University of Houston, Houston, TX, 77204, USA.

sitivity. The stimulus value can then be recovered by looking at the simultaneous activity of all of the channels. Coding motion direction and velocity by relying on comparison between channels makes the system relatively insensitive to other variables, such as color or contrast, that can be expected to affect all of the channels equally (see Regan, 1982). If full-field motion were to be processed by channels, what might they look like and how might we gather evidence about their characteristics? A channel specialized for the detection of full-field rotation-related visual motion would respond optimally to the visual motion resulting from rotation about a particular axis. These hypothetical full-field rotatory-movement channels would respond optimally to a particular distribution of motion over the retina, the pattern normally evoked by eye rotation. When the eye rotates, it causes movement of all of the different parts of the retinal image by an amount proportional to the sine of the angle between the visual direction of a particular point and the orientation of the axis of rotation. Thus, translational retinal motion varies from none for points in line with the axis, to a peak for points orthogonal to the orientation of the axis. The response of a hypothetical full-field rotatory-movement channel would be maximal when the experienced rotation axis was aligned with the axis of maximal sensitivity for that channel and decline as the axis of stimulus rotation deviated from this axis orientation. Such a channel would be insensitive to movement around an axis that was orthogonal to the orientation of the axis to which it was maximally sensitive. There would need to be a minimum of three channels tuned to different axis orientations so that it would not be possible for rotation to be about an axis orthogonal to all of the channels. More than three channels would be redundant since space is three dimensional.

Evidence for a visual attribute being processed by a channel-based system can be obtained by a number of techniques (Regan, 1982). Here we have looked at the variations in the lower motion threshold for detection of rotation about axes of different orientations. We used an analogy with color vision research where variations in the thresholds to monochromatic light yield important cues about the organization of the processing system (Cole et al., 1993). The organization of a channel-based system might lead to anisotropies in the distribution of detection thresholds for motion in different directions (Regan, 1982; Campbell & Tedeger, 1991; Howard, 1991). Intriguing examples of psychophysical and physiological directional anisotropies for motion in the fronto-parallel plane have been reported (Georgeson & Harris, 1978; Regan & Price, 1986; Albright, 1989; Raymond, 1994) but have not been investigated using full-field stimuli.

Systems for processing full-field rotation-related visual motion by small sets of neurones tuned to particular directions (Oyster et al., 1972) or particular rotation axes (Simpson et al., 1989) have been proposed for the control of the brain-stem-controlled visual reflex, optokinetic nystagmus in the rabbit (Simpson, 1984; Tan et al., 1993). However, the visual information that powers optokinetic nystagmus in humans originates largely in the cortex (Harris et al., 1993) which suggests the possibility of perceptual correlates. In this paper, we report the movement detection thresholds for the detection of rotation around a range of axes. We have determined the lower motion threshold that is the lowest speed that can be distinguished from stationary. There are significant variations among axes. The distribution of thresholds is compatible with a three-channel system for processing visual movement. Some of these data have been presented in preliminary form (Harris & Lott, 1993, 1994; Lott & Harris, 1993).

Methods

Subjects

Three subjects participated in the experiment. Their ages ranged from 20 to 30 years, and each had normal vision with no history of strabismus or other visual disorders. Two subjects were naïve to the experimental hypotheses and were paid for their services, and the third was one of the authors (LL). All subjects gave their informed consent.

Apparatus and visual stimulus

The stimulus was a pattern of dots projected by a planetarium projector onto a 57-cm radius hemispherical screen (see Fig. 1). The dots were generated by shining a single projector bulb through pin holes made with a random distribution in a 10-cm-diameter metal sphere that surrounded it. Each projected dot subtended approximately 4 deg × 3 deg on the screen and had fuzzy edges. The density of the dots was approximately 26 dots/m^2. The planetarium projector was the only source of light illuminating the screen. When the projector was on, the luminance of the dots and background were 11.56 cd/m^2 and 1.54 cd/m^2, respectively. This resulted in a Michelson contrast, defined as $(L_{max} - L_{min})/(L_{max} + L_{min})$, of 0.76. The projector could be rotated at velocities of between 0.04 deg/s and 74 deg/s with a resolution of 0.02 deg/s under 12-bit computer control through a Cambridge Electronic Design 1401 interface box. The rotation axis of the projector could be positioned, also under computer control, with ±0.5 deg accuracy.

Subjects sat at the center of the dome. Their knees and hands which held the response buttons were below the screen and were not visible. Subjects were positioned by eye with their Frankfurt plane (defined as the plane containing the ear canal and the suborbital bone) approximately horizontal. This is close to the comfortable natural resting position of the head. A chin rest was used to maintain the subject's head position. In this position, the subject's eyes were 12 cm below the geometric center of the screen and the planetarium projector was centred 5 cm above the geometric center (see Fig. 1). A red LED was mounted on the far side of the hemisphere at the center (see Fig. 1). The LED, viewed through the translucent material of the screen, served as a fixation point in between stimulus presentations.

Definition of coordinate system

Each stimulus rotation axis is described as a vector in a polar system of eccentricity and direction (Figs. 2B and 2C). *Eccentricity* is defined as the angle between the rotation vector and the direction of the fixation point. An eccentricity of 0 deg corresponds to the axis passing through the fixation point (roll—Fig. 2B), 90 deg corresponds to an axis in the fronto-parallel plane, and so on. *Direction* is defined as the angle between a vector pointing straight down (yaw axis—Fig. 2C) and the projection of the rotation vector onto a fronto-parallel plane. In our convention, a positive axis direction corresponds to a displacement from the straight down in the counterclockwise direction. Thus, a direction +90 deg corresponds to an axis coming out of the subject's right ear. The polarity of the rotation about the vector is described by a left-hand rule. Rotation polarity is found by lining up the left thumb with the vector pointing out from the center of the head. The fingers then curl in the direction of rotation.

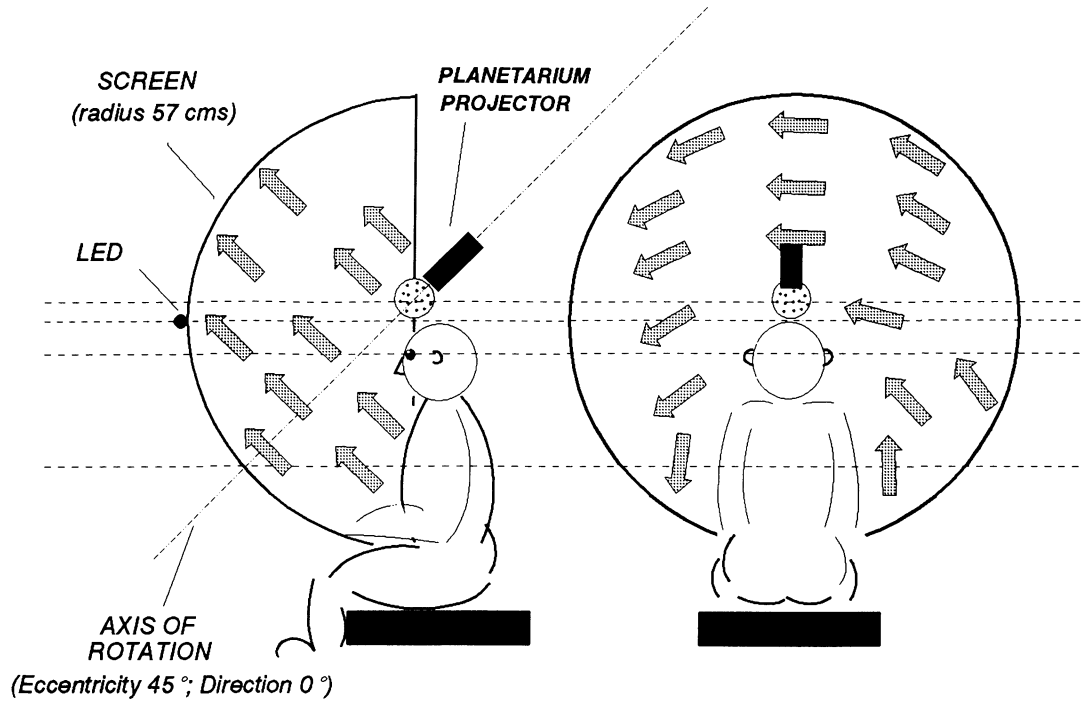

Fig. 1. The equipment. The subject sat in a 57-cm-radius hemispherical screen with their eyes 12 cm below the geometric center. A planetarium projector was positioned directly above the subject with its center 5 cm above the geometric center. An LED was positioned on the dome opposite the geometric center. The projector could rotate around any axis. The gray arrows represent the direction of movement of the projected dots for one particular orientation of the projector (eccentricity 45 deg; direction 0 deg—see Methods for convention) when seen from the left side (left side of figure) or from behind (right side of figure). The horizontal dashed lines indicate from top to bottom, the height of the planetarium, fixation point, eyes and the intersection of the axis of rotation with the screen.

Thus, direction = 0 deg, eccentricity = 0 deg corresponds to roll with the spots moving counterclockwise around the location of the fixation point. Direction = 0 deg, eccentricity = 180 deg corresponds to the same axis but with the spots moving clockwise. Similarly, direction = 0 deg, eccentricity = 90 deg corresponds to rotation about the subject's yaw axis (Fig. 2) with the spots straight ahead moving to the left, and direction = 180 deg, eccentricity = 90 deg corresponds to yaw axis rotation with the straight ahead spots moving to the right. Direction = 90 deg, eccentricity = 90 deg corresponds to rotation about the subject's pitch axis with the central spots moving down, and direction = 270 deg, eccentricity = 90 deg corresponds to pitch with central spots moving up.

Only axis orientations in the lower right quadrant were used, that is directions 0 deg to 90 deg with eccentricities 0 deg to 90 deg and directions 180 deg to 270 deg with eccentricities 90 deg to 180 deg. This restriction was because the system used for positioning the axis involved a guide-track on the right-hand side which cast an earth-stationary shadow when it was between the bulb and the screen.

Procedure

Movement detection thresholds were measured for 29 axes (see Fig. 3). All measures were obtained under binocular viewing conditions. Subjects kept their chin in the chin rest and maintained fixation on the LED when it was illuminated. Prior to each trial, the fixation spot disappeared and subjects were instructed to keep looking at that area of the screen throughout the 3-s trial.

Each trial consisted of two 1-s intervals separated by 1 s. The dot pattern moved continuously at a constant velocity during one period and was stationary in the other. The screen was dark during the interstimulus interval. A two-alternative forced choice (2AFC) with a transformed up–down method was used (Wetherill & Levitt, 1965; Levitt, 1971). Subjects indicated which interval contained movement by pressing one of two buttons. Two correct responses in a row resulted in a 20% decrease in velocity, and one incorrect response caused velocity to be increased by 20%. The mean of the last four out of eight reversals was taken as threshold. This regime provides an estimate of the 70.7% correct detection point (Wetherill & Levitt, 1965).

Five rotation axes were tested in each 50-min session. Each axis position included both rotation polarities for a total of ten separate threshold measures per session. Subjects participated in a total of 18 50-min sessions. Three threshold estimates for each rotation axis were obtained for each subject. The order of presentation was randomized with the constraint that a given rotation axis was never tested more than once in the same session.

Data analysis and modelling

The mean and standard deviations of the three estimates of threshold for each of the 29 tested rotation axes were calculated for each of the three subjects for each rotation polarity. A best fit to the distribution of thresholds was calculated using a model

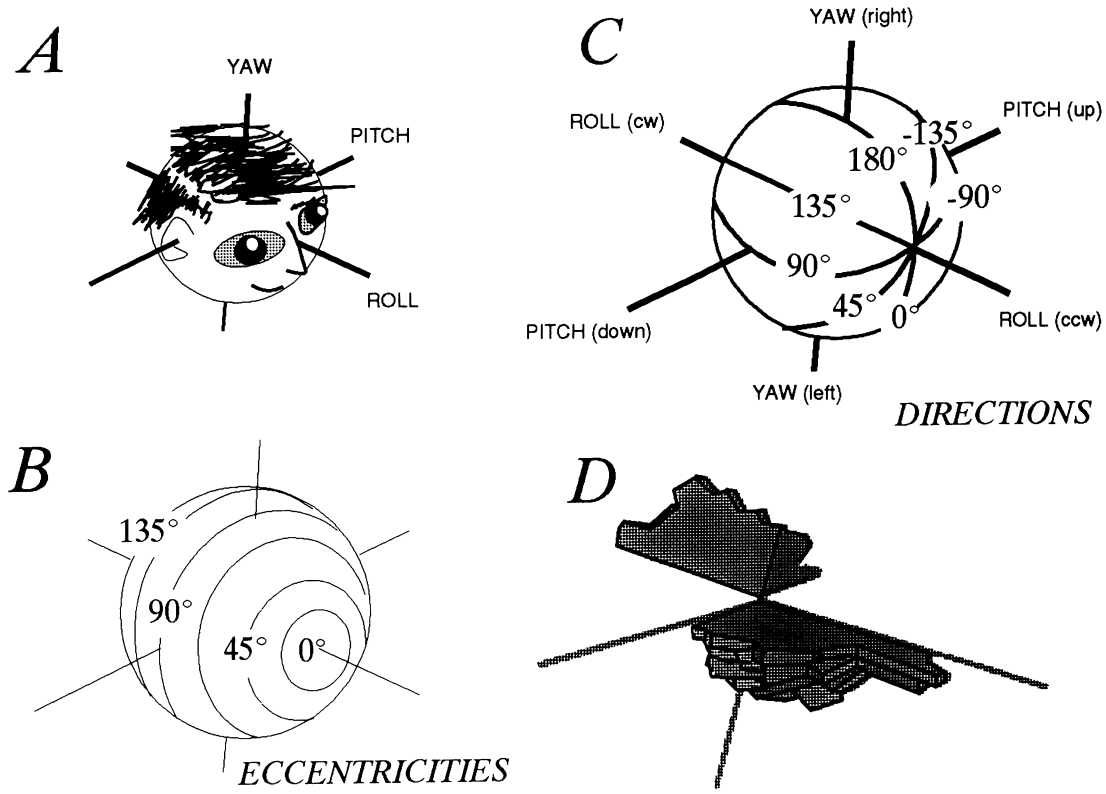

Fig. 2. The nomenclature to describe the orientation of the axes. Fig. 2A shows the cardinal axes of rotation of a person: yaw, pitch, and roll. The subject can be conceived of as sitting in the center of a sphere. The possible axes of rotation are then identified by noting the point at which the axis passes through the sphere. This point is described by two numbers: the eccentricity (the angle between the point and the roll axis—Fig. 2B) and the direction (the angle between a vector pointing straight down and the projection of the rotation vector onto a fronto-parallel plane—Fig. 2C). Rotation polarity is then given by a left-hand rule in which the fingers of the left-hand curl in the direction of rotation when the left thumb is aligned with the axis pointing away from the head. Fig. 2D represents thresholds on a three-dimensional plot where the distance from the center in the direction of each test axis represents the threshold value. A tiled surface has been extrapolated between the 29 data points that make up the two tested quadrants (corresponding to the two rotation polarities).

in which full-field rotation is detected by three independent channels. The method follows the work of Quick (1974) as applied by Cole et al. (1993). Each channel is represented by a rotation vector which lies along the axis of rotation to which it is most sensitive. The length of the channel vector is its sensitivity (reciprocal of threshold). The activity of a given channel in response to rotation at any speed about any axis can be calculated as the dot product of the rotation vector with the channel vector:

$$\textit{Output of channel} = [\textit{Channel vector}] \cdot [\textit{Rotation vector}] \tag{1}$$

Thus, the total activity is the sum of the channels:

$$\textit{Total activity} = \sum Abs(\textit{Output of each channel})^p \tag{2}$$

where p = the amount of probability summation, taken as 3. A total activity of 1 corresponds to threshold.

The predicted rotation threshold about any axis can be calculated by solving eqn. (2) for rotation vector length when total activity = 1:

$$\textit{Rotation vector length} = \frac{1}{\sum Abs[\textit{Channel vector}] \cdot [\textit{Unit rotation vector}]^{p\,1/p}} \tag{3}$$

We used a nonlinear minimization algorithm (Powell's method) to find the best arrangement and sensitivity of a set of three channel vectors where the predicted values best described the data.

Given

v_i = measured threshold of the ith data point

o_i = predicted threshold of the ith data point

e_i = standard deviation of the ith data point

the program minimizes the chi-squared calculated as

$$\chi^2 = \sum \frac{(o_i - v_i) \cdot (o_i - v_i)}{(e_i \cdot e_i)} \tag{4}$$

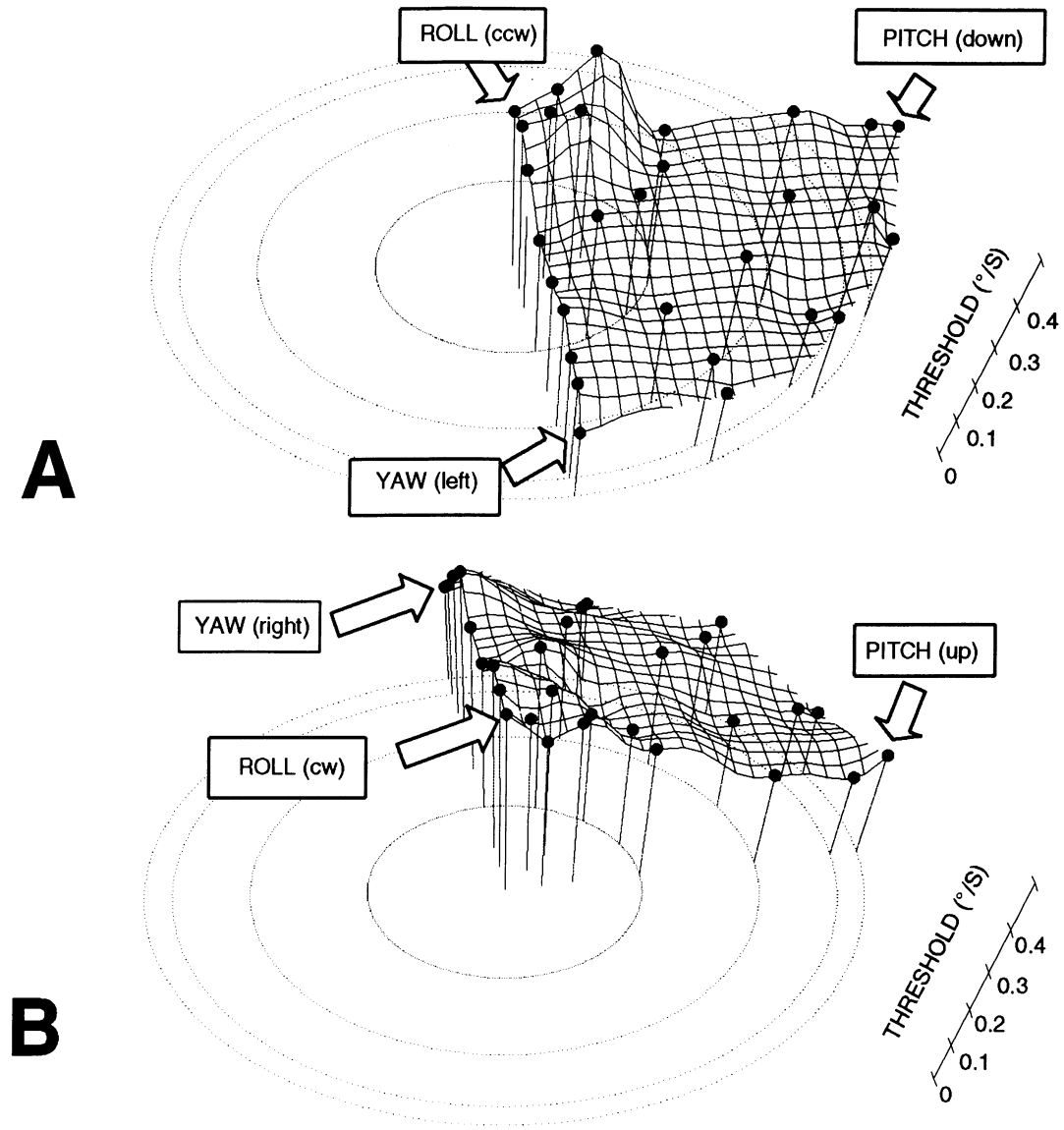

Fig. 3. Thresholds for the detection of motion for all 29 tested axes. The height of each vertical line represents the threshold value. The circles are lines of equal eccentricity, the center of which represents roll rotation (cf. Fig. 2). Fig. 3A shows axes with combinations of counterclockwise roll, leftward yaw, and downward pitch; Fig. 3B shows axes with combinations of clockwise roll, rightward yaw, and upward pitch. The figures have been drawn in perspective which accounts for the tilt of the vertical lines.

Results

Comparison of movement detection thresholds for all axes

Data

There was considerable variation among the responses to rotation about the different axes tested. Threshold velocities for the detection of full-field movement about each of the tested axes are presented in three-dimensional plots (Figs. 2D, 3A, and 3B) and in cross sections through such plots (Figs. 5, 6, and 7) for each of the three subjects.

Mean thresholds were subjected to a 4 (eccentricities: 22, 45, 67, and 90 deg) by 5 (directions: 0, 22, 45, 67, and 90 deg) by 2 (polarities of rotation around the axis) within-subjects analysis of variance (ANOVA) to determine whether the thresholds for these rotation axes were significantly different. This analysis revealed significant main effects of eccentricity [$F(3,6) = 9.45$, $P < 0.02$] and direction [$F(4,8) = 12.36$, $P < 0.002$]. The main effect of rotation polarity was not significant [$F(1,2) = 4.71$, $P > 0.15$]. The interaction of eccentricity and direction was also significant [$F(12,24) = 2.37$, $P < 0.05$] indicating that the effect of eccentricity varies with the different directions: that is, eccentricity-related variations alone are not sufficient to explain the data.

Mean movement detection thresholds varied from 0.139 ± 0.05 deg/s to 0.463 ± 0.166 deg/s. Fig. 2D shows the distribution of mean movement detection thresholds over all of the axes tested (averaged across subjects). Thresholds are represented on a three-dimensional plot where the distance from the center in the direction of each test axis represents the threshold value.

A tiled surface has been extrapolated between the 29 data points that make up each quadrant in Fig. 2D. The sensitivity to rotation about axes close to the line of sight or roll axis (0-deg eccentricity: see Fig. 2D) is lower (thresholds higher) than when the axes are closer to orthogonal to the line of site (90-deg eccentricity: i.e. approaching the yaw/pitch plane). The variation of thresholds with eccentricity does not fully describe the distribution of thresholds. The highest threshold (0.463 ± 0.166 deg/s) was found for rotation about an axis 11 deg off the straight ahead at a direction of 90 deg which was significantly greater than that for straight ahead (0.360 ± 0.177 deg/s: $T = 2.38$; $P = 0.02$ $n = 36$). Fig. 3 plots the motion thresholds for each axis tested. The height of each vertical line represents the threshold value. The circles are lines of equal eccentricity, the center of which represents roll rotation (cf. Fig. 2). Fig. 3A shows axes with combinations of counterclockwise roll, leftward yaw, and downward pitch; Fig. 3B shows axes with combinations of clockwise roll, rightward yaw, and upward pitch. The pattern of variation in threshold across different axes of rotation is very similar for all three subjects.

Simulation by a three-channel model

The data were fit by the output of a three-channel model as described in the Methods section. Fits were obtained to the averaged data and to the data from each individual subject. The model was constrained to fit channels that were symmetrically arranged around the sagittal plane to make the model biologically feasible. The constraints and the orientations of the best-fitting channels are summarized in Table 1. The orientation of a channel refers to the orientation of the axis of rotation to which it is maximally sensitive. The orientations of the best-fit channels are quite similar for each subject. Notice that they are approximately orthogonal and that the sensitivities are not the same for all three channels. Also shown in Table 1 for comparison are the orientations of the semicircular canals.

Fig. 4 plots the orientation of the best-fit axes (Table 1) and compares them with the semicircular canals. In the head position used during this study, the plane of the horizontal canals typically tilts up by about 30 deg (de Beer, 1947; Curthoys et al., 1977). By using eqn. (3), a prediction of the threshold for rotation about any axis can be obtained from the model.

Comparison of movement detection thresholds for axes of constant eccentricity

As the axis of rotation was varied in *direction* whilst keeping *eccentricity* constant, the relative contribution of translation and rotation to the motion of all of the dots at any given eccentricity remained the same. Thus, the thresholds of motion detection around these sets of axes can be compared without the concern that points at a given eccentricity (e.g. the foveal region) might be moving more in some cases than in others. The thresholds to yaw and pitch rotation and for rotation about axes in between are compared in Fig. 5. The format of this and the next two plots (Figs. 6 and 7) are the same. All these plots represent cross sections through the three-dimensional surface of Fig. 2D in the plane shown in the insert. The distance from the center of the plots to each data point represents the threshold for the detection of motion about that axis. The left-hand plot shows individual data points, and the right-hand plot shows the averages and standard deviations. Superimposed on the average data is the thresholds predicted by the best-fit model [obtained from eqn. (3) and the average channel locations and sensitivities given in Table 1].

There was no difference between the two directions of either yaw rotation (viewing binocular: mean threshold: 0.195 deg/s:

Table 1. *The arrangement of channels that best simulate the variation in velocity detection thresholds*[a]

	Channel	Direction (deg)	Eccentricity (deg)	Sensitivity (s/deg)	chi
Symmetry constraints	1	d1	e1	s1	
	2	−d1	e1	s1	
	3	0 (midline)	e3	s3	
Data (all subjects)	1	129.9	75.3	5.75	8.55
	2	−129.9	75.3	5.75	
	3	0	44.9	3.41	
Data (AV)	1	128.3	80.1	7.2	34.12
	2	−128.3	80.1	7.2	
	3	0	19.7	2.9	
Data (LL)	1	123.8	96.5	6.4	44.7
	2	−123.8	96.5	6.4	
	3	0	16.4	2.2	
Data (SK)	1	129.5	64.2	4.7	18.4
	2	−129.5	64.2	4.7	
	3	0	51.5	3.8	
SCC (30 deg up)	1	116.6	52.2		
	2	−116.6	52.2		
	3	0	60		

[a]These channels were obtained by best-fit to the threshold data using the *symmetry constraints* listed in the first part of this table. The orientation of the channels is given in the coordinate system of the data presentation (direction and eccentricity: see Methods). The orientation of the semicircular canals (SCC; Curthoys et al., 1977) is given in the same reference frame for comparison. Sensitivity is the inverse of threshold. The chi value is an estimate of goodness-of-fit (see Methods).

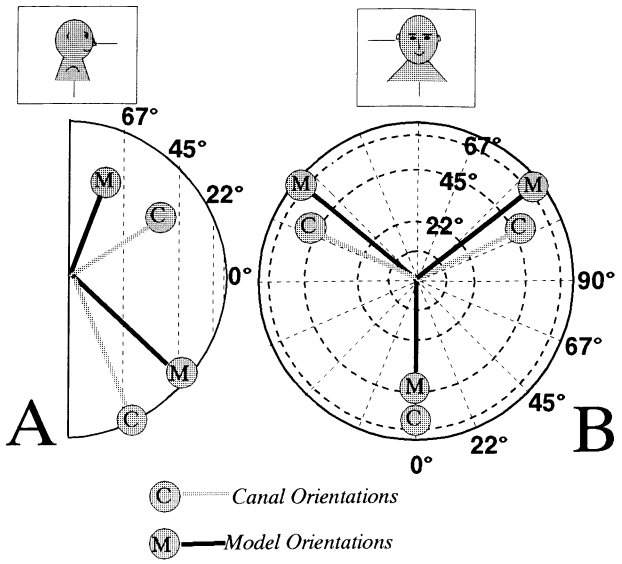

Fig. 4. The orientations of the best-fit model channels (*m*) compared to the orientation of the semicircular canals (*c*). The precise values are given in Table 1. The orientations are shown from the side (panel A) and from the front (panel B). The vertical lines in panel A and the concentric circles of panel B represent *eccentricity* and the radial lines in panel B represent *directions*.

$T = 0.62$; $P = 0.53$; $n = 72$) or pitch rotations (mean threshold: 0.235 deg/s: $T = 0.86$; $P = 0.39$; $n = 36$). The threshold for yaw rotation was significantly lower than for pitch rotation ($T = 4.4$; $P = 0.00003$; $n = 72$). Plotted through the data are the best-fit model predictions (shaded area).

Comparison of movement detection thresholds for axes of constant direction

Figs. 6 and 7 show the variation in detection thresholds as the axis varies from roll to pitch and from roll to yaw, respectively, using the same format as Fig. 5. In this case, the movement of the dots in the central field vary from roll (for roll rotation) through to translation either up and down (for pitch) or left and right (for yaw). There were dramatic differences in these cases in which roll movements were detected only at far higher speeds (0.38 deg/s) than for pitch or yaw rotation (0.24 and 0.20 deg, respectively). The three-channel model fits are also shown.

Variation with eccentricity

Although not all thresholds measured for rotation around axes of any one eccentricity are the same, the major variations are correlated with eccentricity.

Fig. 8 graphs the variation of threshold with eccentricity when all directions are pooled for each eccentricity. There is an apparently linear correlation between threshold velocity and eccentricity of the axis given by

$$\textit{Threshold velocity} = -0.002 \cdot \textit{ecc} + \textit{threshold}_{\textit{ecc}=0\ \text{deg}} \quad (5)$$

where *ecc* is the eccentricity of the axis (Fig. 2) and $\textit{threshold}_{\textit{ecc}=0\ \text{deg}}$ is the detection threshold at *ecc* = 0 deg (about 0.4 deg/s). The slope of this function is −0.002 deg/s per degree of eccentricity.

The same data are plotted in polar coordinates in Fig. 9. Notice that all directions have been collapsed for each value of eccentricity so that while *ecc* = 0 corresponds to ROLL rotation, none of the other points correspond to a single axis of rotation. This method of plotting the data is useful because values

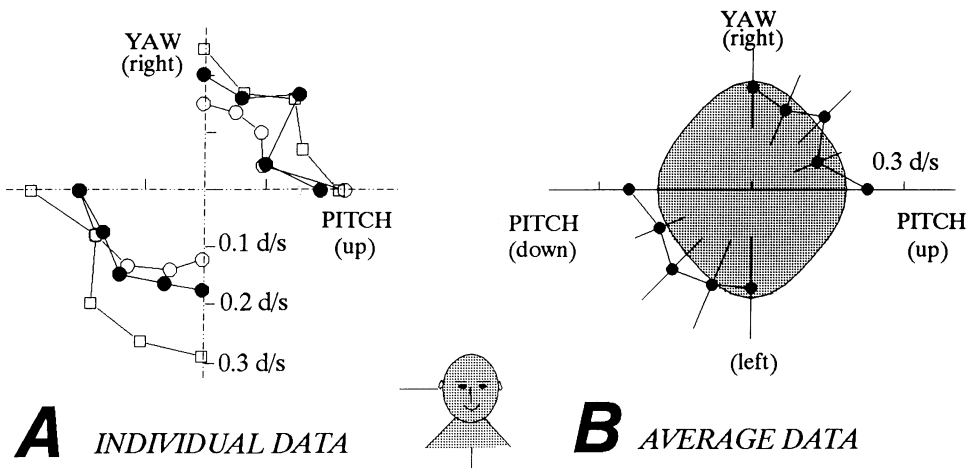

Fig. 5. The threshold velocity for axes between YAW and ROLL. This is essentially a cross section through the detection surface of Fig. 2D in the transverse plane of the head. The orientation of the plane is shown in the insert. All axes are defined with respect to the head. The direction of rotation (left, up, etc.) is described in terms of the rotation of dots directly ahead of the subject. The figure shows the thresholds for the detection of full-field visual rotation (individual subjects panel A; averaged panel B) and compares them to the output of the three-channel model (shaded zone, see text; values as in Table 1). In each graph, the distance of each symbol from the center represents the threshold rotation velocity. The direction of the data point from the center represents the orientation of the axis of rotation. Each data point in panel A represents the mean of three repetitions in each of three subjects, each data point in panel B shows the average of these three values. Also shown in panel B are the standard deviations.

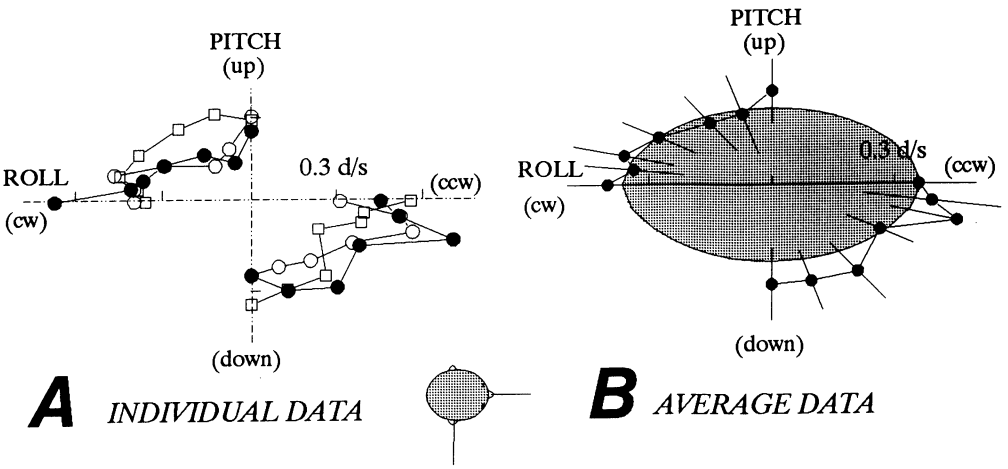

Fig. 6. The threshold velocity for axes between PITCH and ROLL. Conventions are as for Fig. 5.

of thresholds associated with constant amounts of translation in the foveal region fall on the straight dashed lines (see Discussion).

Discussion

This study has shown a variation in thresholds for the detection of full-field visual rotation around various axes. There was no movement in our stimuli except that normally present during pure rotation of the eye. There were no earth-stationary targets or parts of the body visible. When the rotation axis of the stimulus was close to the line of sight, rotation needed to be faster by about a factor of two to three before it was detected than when rotation was about an axis orthogonal to the line of sight (e.g. roll or yaw). Thresholds varied from 0.14 to 0.46 deg/s with the orientation of the rotation axis. The variation of thresholds with axis orientation can be well described by the output of a three-channel visual detection model.

Comparison with detection of patches of motion

Threshold values

Can we predict the detection thresholds for full-field rotation about these various axes from a knowledge of the response to patches of motion? To compare our threshold speeds with those reported in other studies, apart from the obvious differences in stimulus size and extent, also requires paying careful attention to two important features: firstly, the presence of earth-stationary reference points (including the edges of the screen or parts of the subject's body); and secondly, the exposure time of the stimulus. Motion in the absence of reference points might be detected not by motion *per se*, but by detecting when the pattern has moved through a fixed displacement (Kinchla,1971; Snowden, 1992). Thus, smaller displacements (and, apparently, slower speeds) can be detected if the stimulus is on for longer. This is reminiscent of the Mulder constant for the perception of physical angular acceleration by the ves-

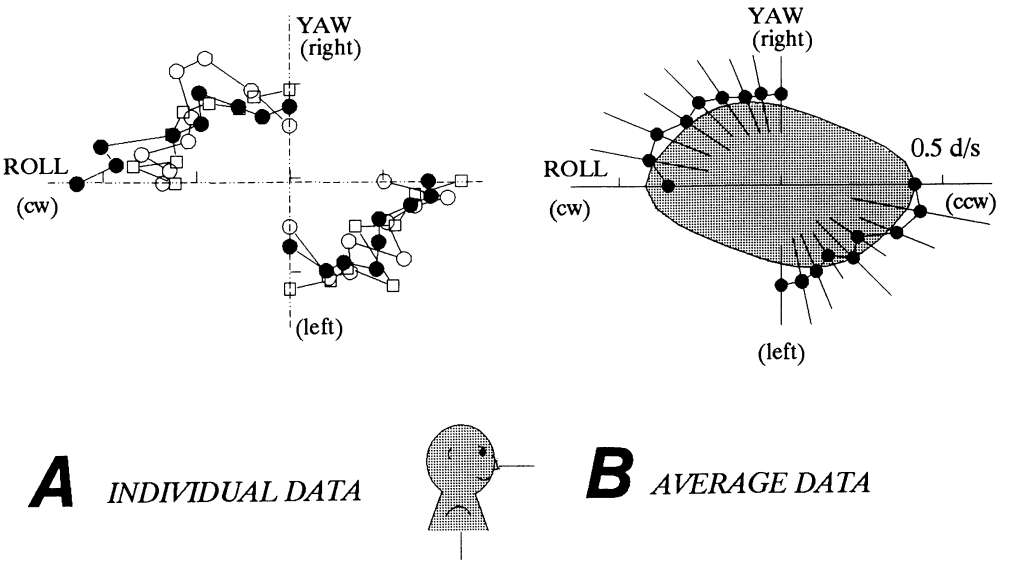

Fig. 7. The threshold velocity for axes between YAW and ROLL. Conventions are as for Fig. 5.

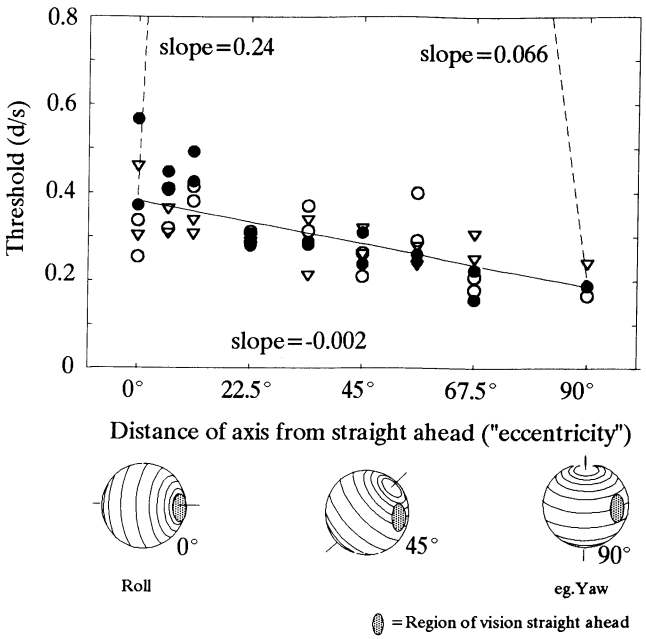

Fig. 8. The variation in threshold with the distance of the axis from the straight ahead (eccentricity). Each symbol represents the average of all directions for each value of eccentricity. Subjects and rotation polarity have been kept separate. Plotted through the data is the best linear fit. The slope is −0.002. The inserts below the horizontal axis illustrate the consequences of eccentricity of the axis of rotation on motion in the foveal region (straight ahead, shaded patch). Also shown are the curves predicted if maximum translation movement (absolute: slope = 0.066) or maximal relative motion (relative: slope = 0.24) were limiting motion detection under these conditions (see Discussion).

tibular system which indicates that lower values of acceleration can be detected if they are maintained for longer (Rodenburg et al., 1981). Our stimuli were presented for 1 s during which time they would have moved through between 8.4 and 27.6 min of arc (corresponding to speeds of 0.14 to 0.46 deg/s) at threshold. This is quite close to values reported by Johnson and Scobey (1982, around 5 min of arc, but the edge of the screen was visible in their case) and Henderson (1971, around 15 min of arc).

Comparison with detection of patches of motion

Variations with eccentricity

All of the stimuli used here have the same distribution of motion over the hemispherical screen. For rotation about any axis, one point on the screen, opposite the end of the axis, purely rotates. If there were a circular dot at the end of the axis, then the rotation of this dot about its center would give no clue to any movement present anywhere in the stimulus. All of the other dots have a varying amount of translation across the screen and across the retina, proportional to the sine of their angular displacement from the axis of rotation, reaching a maximum for the equatorial band of dots orthogonal to the axis of rotation. This distribution is the case for each and every stimulus used here, the only difference among the different axis orientations is which part of the pattern falls on which part of the retina.

If the pattern were to be detected by the translation of each of its component dots independent of the other dots on the screen, then if any particular dot moved by more than the threshold amount for that part of the retina onto which that dot's image fell, it would lead to detection of motion in the pattern. The easiest pattern to detect should, by this logic, be the

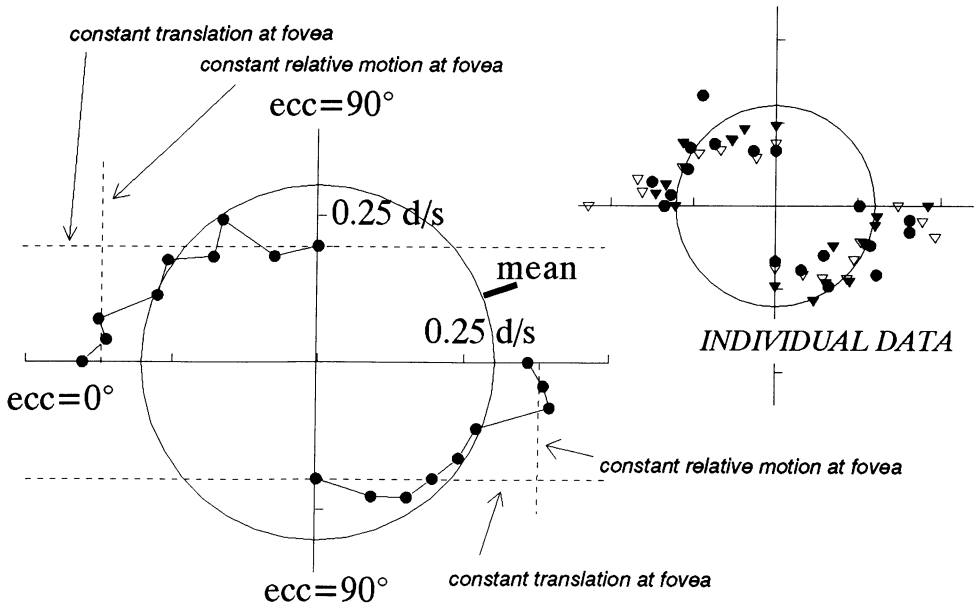

Fig. 9. The variation in threshold with the distance of the axis from the straight ahead (eccentricity) plotted in polar coordinates. The distance of each symbol from the center represents the threshold rotation velocity. The direction of the data point from the center represents the orientation of the axis of rotation. The insert shows the individual data. The data are the same as for Fig. 8 with all directions pooled. Also shown are horizontal dashed lines that represent rotation speeds where the dots on the fovea would have the same amount of translation. This line predicts lowest thresholds (comes closest to the center) for *ecc* = 90 and reaches infinity at *ecc* = 0 when there is NO translation on the fovea. The vertical dashed lines represent rotations speeds where the dots on the fovea have the same amount of relative movement in the fovea. This line predicts the lowest thresholds at *ecc* = 0 where there is the maximum amount of shear between the stationary dot at the end of the axis and its neighbors. Infinite thresholds are predicted at *ecc* = 90.

one with the most translation of dots at the most sensitive part of the field, the fovea. Indeed this is the case: rotations about axes of an eccentricity of 90 deg (see Fig. 2) tend to be detected with the lowest thresholds (around 0.2 deg/s). Similarly, rotation about other axes should be detected when the translation of any of the component dots reaches threshold for that part of the retina on which their images fall. As the orientation of the rotation axis varies from an eccentricity of 90 deg (e.g. yaw or pitch) through to eccentricity of 0 deg (roll: see Figs. 5–9), the part of the retina on which the image of each dot falls moves correspondingly. If we knew the sensitivity of each patch of retina to translation, therefore, and if detection of motion of the pattern depends on the detection of motion of any of the constituent dots, we ought to be able to predict the detection threshold for each rotation axis.

Various studies have assessed the variation with distance from the fovea of the detection of motion (Tyler & Torres, 1972; Johnson & Leibowitz, 1976; Tynan & Sekuler, 1982; Wright & Johnston, 1985; Wright, 1987) and concluded, with some caveats, that, at least for stimuli that are not limited by contrast sensitivity, the threshold varies approximately with the magnification factor. That is, the variation of threshold with distance from the fovea is given by

$$Threshold = Threshold\ to\ foveal\ motion \cdot (m \cdot dist + 1) \quad (6)$$

where *dist* is the distance of the patch of retina in question from the fovea (in degrees) and m is the magnification factor, around 0.33 (deg^{-1}) (Sakitt & Barlow, 1982). This function has a slope of detection $threshold_{ecc=90} \cdot m = 0.2 \cdot 0.33 = 0.066$. Thus, if the detection of these motions was achieved by detecting motion of the maximally moving dots, the data should have a slope of 0.066. This prediction is plotted in Fig. 8 (curve labelled "slope = 0.066"). Clearly, it does not describe the data. It suggests that the threshold for roll stimuli should be $(0.33 \cdot 90 + 1) = 30.7$ times that of pitch or yaw. In fact rotation around axes of *ecc* = 90 deg have thresholds only about twice as high as for roll stimuli.

Could it be that for a given axis of rotation, although the maximally translating dots (orthogonal to the axis) fall on parts of the retina where their movement is not detected, the motion of the dots on the fovea might be detected? The motion of dots around any axis can be decomposed into two vectors corresponding to *ecc* = 90 deg (rotation with maximal translation at the fovea) and *ecc* = 0 deg (rotation with maximal relative motion at the fovea). If the foveal translation component is to be constant, then

$$Required\ detection\ velocity = \frac{Detection\ threshold_{ecc=90\ deg}}{\sin(ecc)} \quad (7)$$

where *ecc* is the eccentricity of the axis (see Fig. 2) and *Required detection velocity* is the detection threshold at that eccentricity that would be associated with suprathreshold foveal movement.

On a polar plot, this function is a straight line and is shown as the horizontal line labelled "constant amount of translation in the fovea" in Fig. 9. For eccentricities between 90 and 45 deg the data are quite well described by the "constant translation" lines, but beyond that the detection of full-field motion is not achieved by detection of motion at the fovea. When rotation is at threshold velocity with the rotation axis at eccentricities between 0 and 45 deg, there is no dot translation anywhere that is above threshold for that region of retina on which its image falls.

Thus, we can conclude that the detection of motion in our stimuli is not being done on the basis of the motion of individual dots considered in isolation. There are two methods by which the detection system could take into account the other dots on the screen. One is by *integrating* their movement over a large area and the second is by *comparing* their movement. The former is still monitoring movement relative to the subject, the latter is detecting relative movement between the dots on the screen. There is relative motion present in the stimuli despite the absence of earth-fixed visual targets since, as described above, some of the dots are translating more than others. In particular the dot at the end of the axis is not translating at all.

So what if relative movement is being detected? That is the *comparison* option. Sensitivity to relative motion is much better than to so-called absolute motion (Johnson & Scobey, 1982; Snowden, 1992) and also falls off with eccentricity but with a slope steeper than the magnification factor (0.6 deg^{-1}; McKee & Nakayama, 1984). Substituting 0.6 for m and $Detection\ threshold_{ecc=0}$, in eqn. (6) suggests a slope of 0.24. Points in the stimulus close to the axis of rotation have lots of relative motion but very little translation across the retina. Points in the stimulus orthogonal to the axis will have maximal translation and minimal relative motion. If motion of our stimulus was being detected by relative motion, then, as the areas of maximum relative motion move away from the fovea, this would predict a fall off with a slope of 0.24. This function is plotted through the data in Fig. 8 (labelled "slope = 0.24"). Since the thresholds actually IMPROVE rather than DIMINISH as the area of maximal relative motion leaves the fovea, it is an even worse fit to the data than the curve based on the detection of maximal translation.

Using the same argument as used above for translation, rotation speeds for various eccentricities of the axis that are associated with the same amount of relative movement of dots in the fovea fall on the vertical dashed lines of Fig. 9 labelled "constant relative motion at fovea." These describe the data over the range of eccentricities 0 to 22.5 deg only; beyond that there is no relative motion anywhere that is above threshold for that region of retina on which its image falls.

Three channels with different sensitivities

Our data cannot be explained by either their local relative or absolute motion content and we next need to consider the possibility of integration over a larger area. We hypothesize that this could economically be done by a set of three channels each integrating over the entire field and providing a signal whose strength fell off as the sine of the angle between the axis of rotation to which the channel was maximally sensitive and the actual axis of rotation. The actual axis (and velocity) of rotation could subsequently be recovered by comparison of the outputs of the three channels.

We have shown that a reasonable fit to the data can be achieved with such a three-channel system: models based on the independent detection of motion in small patches of the retina cannot explain the data. There would need to be a minimum of three channels tuned to different orientations of their opti-

mal rotation axes so that it would not be possible for rotation to be about an axis orthogonal to all of the channels. More than three channels would be redundant. In fact, the technique employed here of looking at variations of thresholds among axes cannot distinguish between three and more than three channels, since a system employing more than three channels is a redundant system which can be precisely mimicked or metamerized by three channels.

Constructing the channels

Constructing full-field motion visual channels requires putting together detectors that are sensitive to different patterns of movement in different areas of the retina. Detectors for pure translation are required in areas orthogonal to the orientation of the rotation axis to which the channel is maximally sensitive, while detectors responding best to combinations of rotation and translation (curl) are required at other sites. Cells with just these properties have been reported in the medial superior temporal area (MST) of the monkey cortex (Tanaka & Saito, 1989; Duffy & Wurtz, 1991*a*,*b*). However, their distribution does not immediately suggest an organization into three channels. The output of subpopulations of MST cells would be required, selected to provide the building blocks for a given channel. The output of these subpopulations would then correspond to the cortical input to the brain-stem system, especially the accessory optic system (Ungerleider et al., 1984; Boussaoud et al., 1992). The cortical projection functionally dominates the direct retinal projections to the accessory optic system in the control of reflex eye movements in humans (Harris et al., 1993).This route, originating in the cortex, would then determine the visual properties of the accessory optic system and its projections including the inferior olive, cerebellar regions, and vestibular nucleus.

Coding full-field retinal slip in a three-channel system is appealing in its economy and is readily compatible with relevant vestibular information. Comparing the output of three channels might form a convenient way to extract full-field *rotation* information in a visual stimulus that contains both rotational and translational components.

Acknowledgments

This work was funded by a grant from the National Science and Engineering Research Council of Canada to LRH OGP0046271. We would like to acknowledge the generous support of the Institute of Space and Terrestrial Sciences. We would also like to thank William McIlhagga for help with the fitting method and Angelica Velman and Marlou Hacfoort for help with the data collection. Michael Jenkin helped with the graphical presentations of the model and data. We would like to thank Marlou Hacfoort, Andy Smith, and Jane Raymond for helpful comments on an earlier draft of this manuscript.

References

ALBRIGHT, T.D. (1989). Centrifugal directional bias in the middle temporal visual area (Mt) of the macaque. *Visual Neuroscience* **2**, 177–188.

BOUSSAOUD, D., DESIMONE, R. & UNGERLEIDER, L.G. (1992). Subcortical connections of visual areas MST and MT in macaques. *Visual Neuroscience* **9**, 291–302.

CAMPBELL, F.W. & TEDEGER, R.W. (1991). A survey of channels and challenges of information and meaning. In *Channels in the Visual Nervous System: Neurophysiology. Psychophysics and Models*, ed., B. BLUM. London: Freund Publishing House.

CHOUDHURY, B.P. & CROSSEY, A.D. (1981). Slow-movement sensitivity in the human field of vision. *Physiology and Behavior* **26**, 125–128.

COLE, G.R., HINE, T. & MCILHAGGA, W. (1993). Detection mechanisms in L-, M- and S- cone contrast space. *Journal of the Optical Society of America* **10**, 38–51.

CURTHOYS, I.S., BLANKS, R.H.I. & MARKHAM, C.H. (1977). Semicircular canal functional anatomy in cat, guinea pig and man. *Acta Otolaryngolica* **83**, 258–265.

DE BEER, G.R. (1947). How animals hold their heads. *Proc. Linnean Soc.* **159**, 125–139.

DUFFY, C.J. & WURTZ, R.H. (1991*a*). Sensitivity of MST neurons to optic flow stimuli, 1. A continuum of response selectivity to large-field stimuli. *Journal of Neurophysiology* **65**, 1329–1345.

DUFFY, C.J. & WURTZ, R.H. (1991*b*). Sensitivity of MST neurons to optic flow stimuli, 2. Mechanisms of response selectivity revealed by small-field stimuli. *Journal of Neurophysiology* **65**, 1346–1359.

GEORGESON, M.A. & HARRIS, M.G. (1978). Apparent foveofugal drift of counterphase gratings. *Perception* **7**, 527–536.

HARRIS, L.R. (1994). Visual motion caused by movements of the eye, head and body. In *Detecting Visual Motion*, ed. SMITH, A.T. & SNOWDEN, R., pp. 397–436. London: Academic Press.

HARRIS, L.R., LEWIS T.L. & MAURER, D. (1993). Brain-stem and cortical contributions to the generation of horizontal optokinetic eye-movements in humans. *Visual Neuroscience* **10**, 247–259.

HARRIS, L.R. & LOTT, L.A. (1993). Thresholds for full-field visual motion indicate an axis based coding system similar to that of the vestibular system. *Neuroscience Abstracts* **19**, 316.21.

HARRIS, L.R. & LOTT, L.A. (1994). Thresholds for full-field visual motion: Variation with eye-in-head position. *Investigative Ophthalmology and Visual Science* **35**, 2000.

HENDERSON, D.C. (1971). The relationship among time, distance, and intensity as determinants of motion discrimination. *Perception and Psychophysics* **10**, 310–320.

HOWARD, I.P. (1991). Adaptations to transformations of the optic array. In *Presbyopia Research: From Molecular Biology to Visual Adaptation*, ed. OBRECHT, G. & STARK, L., pp. 73–81. New York: Plenum.

HOWARD, I.P. & HOWARD, A. (1994). Vection: The contributions of absolute and relative visual motion. *Perception* **23**, 745–751.

JOHNSON, C.A. & LEIBOWITZ, H.W. (1976). Velocity time reciprocity in the perception of motion: Foveal and peripheral determinations. *Vision Research* **16**, 177–180.

JOHNSON, C.A. & SCOBEY, R.P. (1982). Effects of reference lines on displacement thresholds at various durations of movement. *Vision Research* **22**, 819–821.

JOHNSTON, A. & WRIGHT, M.J. (1985). Lower threshold of motion for gratings as a function of eccentricity and contrast. *Vision Research* **25**, 179–185.

KINCHLA, R.A. (1971). Visual movement perception: A comparison between absolute and relative movement discrimination. *Perception and Psychophysics* **9**, 165–171.

LEVINSON, E. & SEKULER, R. (1976). Adaptation alters perceived direction of motion. *Vision Research* **16**, 779–781.

LEVITT, H. (1971). Transformed up-down methods in psychoacoustics. *Journal of the Acoustical Society of America* **49**, 467–477.

LOTT, L.A. & HARRIS, L.R. (1993). The detection and discrimination of the velocity and direction of full-field motion. *Perception* **22**, 73.

MCKEE, S.P. & NAKAYAMA, K. (1984). The detection of motion in the peripheral visual-field. *Vision Research* **24**, 25–32.

OYSTER, C.W., TAKAHASHI, E. & COLLEWIJN, H. (1972). Direction-selective retinal ganglion cells and control of optokinetic nystagmus in the rabbit. *Vision Research* **12**, 183–193.

QUICK, R.F. (1974). A vector magnitude model for contrast detection. *Kybernetik* **16**, 65–67.

RAYMOND, J.E. (1994). Directional anisotropy of motion sensitivity across the visual-field. *Vision Research* **34**, 1029–1037.

REGAN, D. (1982). Visual information channeling in normal and disordered vision. *Psychological Review* **89**, 407–444.

REGAN, D. & PRICE, P. (1986). Periodicity in orientation discrimination and the unconfounding of visual direction. *Vision Research* **26**, 1299–1302.

RODENBURG, M., STASSEN, H.P.W. & MAAS, A.J.J. (1981). The threshold of perception of angular acceleration as a function of duration. *Biological Cybernetics* **39**, 223–226.

SAKITT, B. & BARLOW, H.B. (1982). A model for the economical encod-

ing of the visual image in cerebral cortex. *Biological Cybernetics* **43**, 97–108.

SIMPSON, J.I., VAN DER STEEN, J., TAN, J., GRAF, W. & LEONARD, C.S. (1989). Representations of ocular rotations in the cerebellar flocculus of the rabbit. *Progress in Brain Research* **80**, 213–223.

SIMPSON, J.I. (1984). The accessory optic system. *Annual Review of Neuroscience* **7**, 13–41.

SNOWDEN, R.J. (1992). Sensitivity to relative and absolute motion. *Perception* **21**, 563–568.

TAN, H.S., VAN DER STEEN, J., SIMPSON, J.I. & COLLEWIJN, H. (1993). 3-dimensional organization of optokinetic responses in the rabbit. *Journal of Neurophysiology* **69**, 303–317.

TANAKA, K. & SAITO, H. (1989). Analysis of motion of the visual field by direction, expansion/contraction, and rotation cells clustered in the dorsal part of the medial superior temporal area of the macaque monkey. *Journal of Neurophysiology* **62**, 626–641.

TYLER, C.W. & TORRES, J.T. (1972). Frequency response characteristics for sinusoidal movement in the fovea and the periphery. *Perception and Psychophysics* **12**, 232–236.

TYNAN, P.D. & SEKULER, R. (1982). Motion processing in peripheral vision. *Vision Research* **22**, 61–68.

UNGERLEIDER, L.G., DESIMONE, R., GALKIN, T.W. & MISHKIN, M. (1984). Subcortical projections of area Mt in the macaque. *Journal of Comparative Neurology* **223**, 368–386.

WETHERILL, G.B. & LEVITT, H. (1965). Sequential estimation of points on a psychometric function. *British Journal of Mathematical and Statistical Psychology* **18**, 1–10.

WRIGHT, M.J. (1987). Spatiotemporal properties of grating motion detection in the center and the periphery of the visual-field. *Journal of the Optical Society of America A—Optics and Image Science* **4**, 1627–1633.

WRIGHT, M.J. & JOHNSTON, A. (1985). The relationship of displacement thresholds for oscillating gratings to cortical magnification, spatiotemporal frequency and contrast. *Vision Research* **25**, 187–193.